Band Structure of Doped Bismuth Using the Shubnikov–de Haas Effect

G. A. ANTCLIFFE AND R. T. BATE
Texas Instruments Incorporated, Dallas, Texas
(Received 13 February 1967; revised manuscript received 6 April 1967)

The band structure of bismuth has been studied using the Shubnikov–de Haas effect. Oscillatory magnetoresistance has been observed in crystals containing up to 0.06 at. % tellurium. The Fermi energy in the most heavily doped crystals was about 95 meV above the bottom of the conduction band at the L point of the Brillouin zone. Extremal values of the cross-sectional areas of the surface and the electron effective masses were combined with measurements of the electron concentration to demonstrate the validity of the two-band models of Lax and Cohen below about 65 meV. Above this energy there are significant deviations from these models as regards both the cross sections and the effective masses. Thus in heavily doped bismuth, where the Fermi energy is relatively large, the two-band models must be modified. The experimental data reported here may be explained most simply in terms of a two-band model in which the mass at the band edge increases with Fermi energy. A distortion of the Fermi surface above about 70 meV is also reported. The amount of distortion apparently increases more rapidly than predicted by the nonellipsoidal nonparabolic model.

INTRODUCTION

THERE has been much experimental and theoretical effort directed toward a complete determination of the bismuth band structure. At the present time, the following details are well established. The conduction band edges are located at L, the centers of the pseudohexagonal faces of the Brillouin zone, and are characterized by a Fermi surface which is highly elongated. The surface may[1,2] or may not[3,4] be ellipsoidal. The band is highly nonparabolic at the Fermi energy of pure bismuth.[5,6] de Haas–van Alphen measurements[7] provide support for Cohen's nonellipsoidal nonparabolic (NENP) model[3] at energies slightly above the Fermi energy in the pure semimetal, while Shubnikov–de Haas data suggest a uniform decrease in the dimensions of the Fermi surface below this energy.[2] Such experiments indicate that the technique of varying the Fermi level by impurity doping[8–10] can lead to new and important results. This has been recently confirmed by the observation of additional electron bands in tellurium doped bismuth.[11] This approach has also been adopted to investigate both conduction and valence bands in tin-doped bismuth.[12]

The present paper reports the results of a study of the bismuth conduction band using the Shubnikov–de Haas technique. Tellurium was used as the dopant to increase the electron concentration to 2.0×10^{19} cm^{-3} before the oscillatory component of the conductivity vanished below 30 kG. The effects of doping were measured by the high-field ($\omega_c\tau\gg1$) Hall coefficient which for a closed surface is proportional to $(n-p)^{-1}$, where n and p are the electron and hole concentrations, respectively. The angular dependence of the oscillatory period was also investigated, generally with the magnetic field **H** in the binary plane. With this geometry, the shape of the constant energy surfaces may be studied most directly. At the higher doping levels, the interpretation of the experimental data was simplified because the oscillations due to the principal ellipsoid were predominant. The analysis of the low-field data was more straightforward than that taken at higher fields since a single period could usually be isolated.

We may summarize the results of this study as follows. Cohen's NENP model[3] is found to provide a good description of the energy dependence of the conduction-band structure below about 65 MeV. At higher Fermi energies our results indicate that, if the band structure is assumed to be unaffected by doping, the two-band models[3,5,6] no longer provide an adequate description of the conduction band. A pronounced energy-dependent distortion of the quasiellipsoids may also occur at these high Fermi energies.

EXPERIMENTAL

The single crystals from which the samples were cut were grown from tellurium doped melts by the Czochralski method. The maximum tellurium concentration employed was 0.06 at. %. There was no evidence of any gross crystal distortion due to the impurity content. It has been shown[12] that the lattice parameters of bismuth are unchanged by additions of 0.1 at. % tellurium. Representative slices of each ingot were cleaved to determine the approximate direction of the trigonal axis and the ingots were then oriented by back reflection Laue photographs to an accuracy of $\pm1°$. The dimensions of our samples were $10\times2\times1.5$ mm, which was sufficiently small compared to the size of the ingot to assume that each was relatively homogeneous,

[1] E. P. Vol'skii, Zh. Eksperim. i Teor. Fiz. **46**, 2035 (1964) [English transl.: Soviet Phys.—JETP **19**, 1371 (1964)].
[2] R. N. Bhargava, Bull. Am. Phys. Soc. **11**, 330 (1966).
[3] M. H. Cohen, Phys. Rev. **121**, 387 (1961).
[4] V. S. Edel'man and M. S. Khaikin, Zh. Eksperim. i Teor. Fiz. **49**, 107 (1965) [English transl.: Soviet Phys.—JETP **22**, 77 (1966)].
[5] B. Lax, Rev. Mod. Phys. **30**, 122 (1958).
[6] B. Lax, Bull. Am. Phys. Soc. **5**, 167 (1960).
[7] D. Weiner, Phys. Rev. **125**, 1226 (1962).
[8] T. Morimoto, J. Phys. Soc. Japan **21**, 1008 (1966).
[9] K. Tanaka, J. Phys. Soc. Japan **20**, 1633 (1965); **20**, 1374 (1965).
[10] T. Yamada, J. Phys. Soc. Japan Suppl. **21**, 726 (1966).
[11] G. A. Antcliffe and R. T. Bate, Phys. Letters **23**, 622 (1966).
[12] P. Cucka and C. S. Barrett, Acta Cryst. **15**, 865 (1962).

TABLE I. Characteristics of doped bismuth alloys.

Sample	Mobility (10^5 cm^2/V sec) μ_3	$\frac{1}{2}(\mu_1+\mu_2)$	$\left(\frac{1}{\Delta H}\right)^{-1}=f$ (10^5 G)	m^*/m_0	N (10^{18} cm^{-3})	E_f (meV) From f	From m^*/m_0	From f/m^*
57 1-1	3.34		0.192	0.0110	0.70	33.3	32.2	33.7
48 1-1		2.88	0.256	0.0129	1.01	39.5	39.5	39
47 0-5	1.19				2.75			
47 3-2	0.95		0.61	0.020	3.27	64.5	64.5	63
47 4-2			0.76	0.022	4.35	72.5	72	71.5
47 4-1	0.75		0.77	0.0225	5.00	78	85.5	74
05 1-1			0.91	0.0258	6.01			
47 1-3	0.49		1.11	0.030	8.60	89.5	100	77.5
47 1-1	0.36		1.23		8.60	94		
05 1-2			1.15	0.030	8.70	91	100	82
49 3-1	0.42		1.31		9.05	97.5		
49 2-1	0.37		1.45	0.035	11.5	103	118	88
49 1-1			1.75	0.0405	14.2	113	138	92
53 1-0	0.14				32.0			
53 2-0	0.085				41.5			
53 3-0	0.083				46.0			

This was confirmed by the observation of strong oscillatory conductivity from all samples.

A sensitive derivative recording technique[13] was used to detect the small signals encountered in this study. No dependence on the dc measuring current flowing in the sample was observed for currents up to 500 mA. Magnetic fields of up to 30 kG were provided by a superconducting solenoid. The samples were rotated in this magnetic field by a gear arrangement in the helium cryostat. Measurements were carried out mainly at 1.25°K.

RESULTS

The characteristics of the samples studied are listed in Table I. As the tellurium content is increased, the electron concentration increases while the mobility drops due to the increase in both the effective mass and the amount of impurity scattering. It has been shown that, provided the hole concentration is zero,[7,14] one tellurium atom produces one conduction electron.[15] The values of the mobility[16] along the trigonal axis and in the trigonal plane, denoted by μ_3 and $\frac{1}{2}(\mu_1+\mu_2)$, respectively, were measured by the quantity $R_\infty\sigma$, where σ is the appropriate conductivity. Figure 1 shows the magnetic field dependence of R for two representative samples and two directions of magnetic field. For all our samples, the high-field plateau for the Hall coefficient could be obtained below 30 kG. It has been shown[11] that above about 55 meV, other electron bands are populated to the extent of about 3% of the total electron concentration. The mobility of such electrons is not

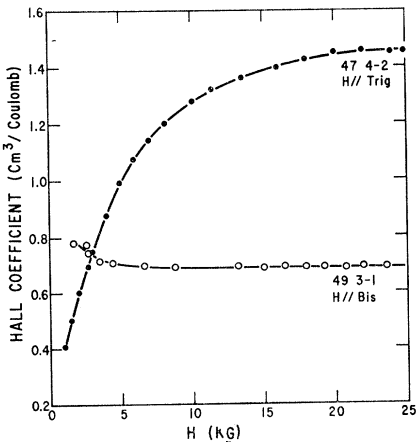

FIG. 1. Typical magnetic field dependence of the Hall coefficient for two directions of H and two different electron concentrations. The high-field plateau was obtainable for all samples listed in Table I.

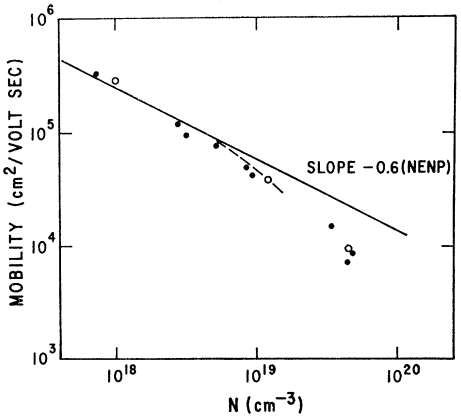

FIG. 2. Electron mobility as a function of the number of electrons N in the conduction band centered at L. Experimental values of μ_3 are denoted by ○ and values of $1/2(\mu_1+\mu_2)$ by ●. The solid line is based on the NENP model and the dashed line indicates the decrease in mobility which would result from the anomolous mass increase reported in the text.

[13] R. T. Bate and N. G. Einspruch, Phys. Rev. **153**, 796 (1967).

[14] A. L. Jain and S. H. Koenig, Phys. Rev. **127**, 442 (1962).

[15] B. H. Schultz and J. M. Noothoven van Goor, Philips Res. Rept. **19**, 103 (1964).

[16] R. N. Zitter, Phys. Rev. **127**, 1471 (1962).

known exactly, although it must be relatively high, since oscillatory effects due to these electrons have been observed. We have assumed here that their mobility is equal to that of the electrons in the conduction band. In this case, $R_\infty\sigma$ measures the carrier mobility exactly. However, the electron concentration in the main conduction band must be reduced from the measured value of R_∞^{-1} by 3%. This concentration will be denoted by N. The decrease in μ_i with increasing N (Fig. 2) shows that both mobilities could be equally well described by a relation of the form $\mu_i \propto N^{-0.9}$. No oscillations were observed for $N > 2\times10^{19}$ cm^{-3} but the mobilities are shown for these samples to indicate the trend. For all but the most lightly doped sample, the hole concentration was negligible. In this case, the electron concentration was estimated from the NENP expression given in the Appendix. This method will be justified in the following section, where we show that this model is valid at low energies. A relation of the form $\mu \propto n^{-0.7}$ has been reported,[14] but we consider that this determination may be based on insufficient experimental data to provide a reliable value of the exponent. The significance of the numerical value of this exponent will be discussed in the following section.

The most important change brought about by tellurium doping is the increase in the dimensions of the Fermi surface. Earlier results[7] suggest that this increase occurs uniformly for additions up to 0.006 at. % tellurium. Direct observation of each dimension of the surface is very difficult or impossible in doped crystals because of the heavy electron masses encountered as **H** approaches the trigonal axis. The reciprocal of the Shubnikov–de Haas period, $f=(\Delta 1/H)^{-1}$, is a direct measure of the extremal cross section S of the Fermi surface cut by a plane normal to the direction of H. In the present investigation between five and ten conductivity minima were usually available to determine an average value for each oscillatory period.

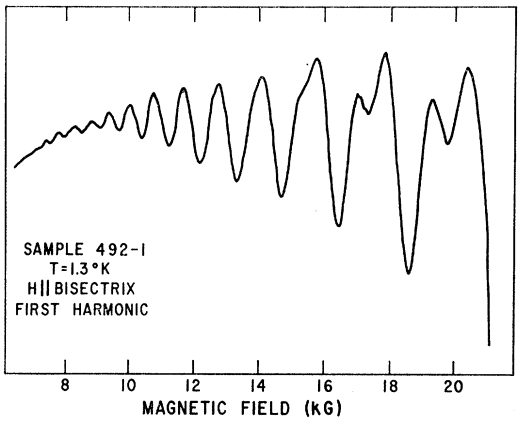

FIG. 3. Photograph of an x-y recording of the first derivative of sample resistance with respect to **H**. Here **H** is || to a bisectrix axis. Electron concentration 1.15×10^{19} cm^{-3}. An increase in sensitivity of about 10× is available to accentuate low-field oscillations.

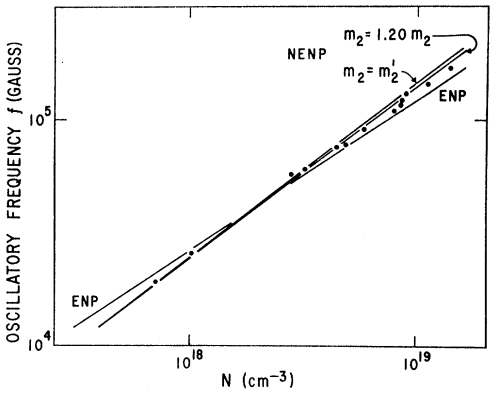

FIG. 4. Increase of the "waist" cross section of the Fermi surface measured by the Shubnikov–de Haas frequency f with increasing electron concentration. **H**||bisectrix axis. Theoretical curves for the ENP and the NENP ($m_2=m_2'$ and $m_2=1.2m_2'$) are indicated.

For **H** parallel to the bisectrix axis, the minimum value of both the extremal cross section and effective mass of a "principal" ellipsoid is obtained. In this orientation the remaining two ellipsoids are equivalent. A photograph of a typical x-y recording for **H** in this orientation is given in Fig. 3. These oscillations are not visible above the monotonic background if the magnetoresistance is measured directly. At low fields, the oscillations (Fig. 3) are due only to the principal surface allowing a unique determination of the period. At higher fields the secondary ellipsoids contribute a period very close to twice that due to the light mass electrons. With **H** parallel to the bisectrix axis, the frequencies due to the principal surface are given in Table I and shown as a function of N in Fig. 4. Values of electron effective mass m^* with **H** parallel to the bisectrix axis were measured by observing the variation of the oscillatory amplitude at constant **H** as a function of temperature below 4.2°K. The temperature enters the theoretical expression for the amplitude[17] through a term which is of the form $\mu/\sinh\mu$, where $\mu=2\pi^2kT/h\omega_c$. The cyclotron frequency $\omega_c=e\mathbf{H}/m^*c$. Values of m^* for the principal surface are listed in Table I and are shown in Fig. 5. No effects which could be attributed to heavy electron oscillations were observed during the determination of m^* from the low-field data. The solid curves in Figs. 4 and 5 have been calculated from the ENP and NENP expressions given in the Appendix [Eqs. (A3)–(A7)]. It has been assumed that $E_g=15$ meV[18] and that the Fermi energy in pure bismuth is 25 meV.[18] The cyclotron masses in pure bismuth are those measured by Kao.[19] Also shown in Figs. 4 and 5 are the theoretical curves predicted by the NENP model with $m_2=1.20m_2'$. The significance

[17] E. N. Adams and T. D. Holstein, J. Phys. Chem. Solids **10**, 254 (1959).
[18] R. N. Brown, J. G. Mavroides, and B. Lax, Phys. Rev. **129**, 2055 (1963).
[19] Y. H. Kao, Phys. Rev. **129**, 1122 (1963).

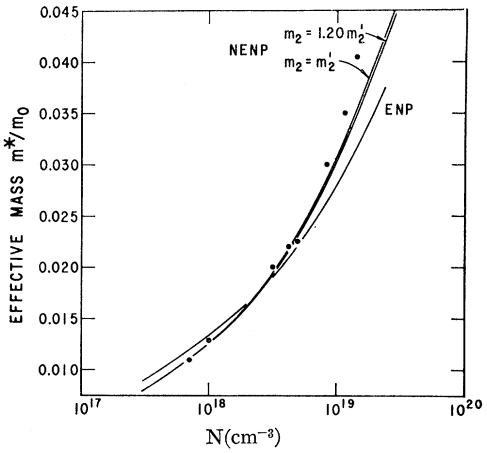

FIG. 5. Increase of electron effective mass m^*/m_0 with increasing electron concentration. The theoretical curves for the NENP model with $m_2=m_2'$ and with $m_2=1.2\ m_2'$ are nearly coincident in this figure.

of m_2' is explained in the Appendix and is discussed in the next section. It is sufficient to observe here that below some critical electron concentration, which is about 3×10^{18} cm^{-3}, our results are in good agreement with the two band models. Cohen's NENP formulation, however, provides a slightly superior description of the data. We cannot determine which value of m_2' provides the better fit to our results because of the small difference in the theoretical volume enclosed by the surfaces in each case. Above the critical concentration mentioned above, significant deviations from the predicted behavior are observed. Brandt and Lyubutina[20] have briefly reported de Haas–van Alphen measurements of m^* in bismuth doped with up to 0.04 at. % tellurium. Their results are presented only as a function of tellurium concentration and so cannot be directly compared with the present data.

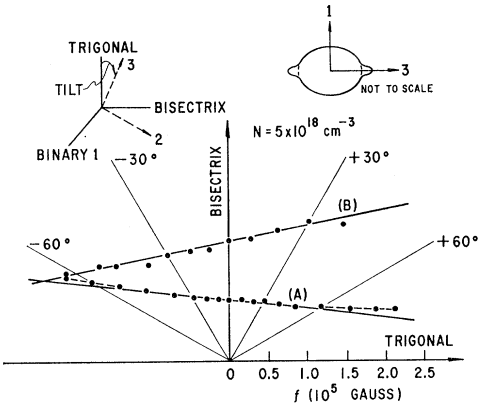

FIG. 6. Angular variation of f due to principle ellipsoid (A) and two equivalent secondary ellipsoids (B) as **H** is rotated in a binary plane. Electron concentration 5.0×10^{18} cm^{-3}. The solid lines represent the theoretical variation predicted by the NENP model with $m_2=m_2'$ or $m_2=1.2\ m_2'$. Also shown are the principal axes in relation to the crystallographic axes and a sketch of the proposed distortion of the surface near the 2-3 plane, which is discussed in the text.

[20] N. B. Brandt and L. G. Lyubutina, in Proceedings of the Tenth International Conference on Low Temperature Physics (to be published).

Although it is not possible to determine each dimension of the surface, a careful study of the angular variation of the extremal cross sections has revealed a nonuniform expansion of the quasiellipsoids. For most of our samples, oscillations were observed with the direction of **H** up to about 65° from the 2-3 plane toward the 2 axis. The principal axis system for each ellipsoid is shown in Fig. 6 in relation to the crystallographic axes which are slightly tilted with respect to them. Figure 6 shows the angular variation of f for both the principal and the remaining two equivalent surfaces with **H** in a binary plane. Linearity on such a polar plot implies that the cross sections are typical of a cylindrical surface extended along the 2 axis. For pure bismuth this is true up to about 75° either side of the 1-3 plane of the surface. For N less than about 3.0×10^{18} cm^{-3} we obtain a similar angular variation to that observed in pure bismuth. At higher concentrations as illustrated by Fig. 5, there is an apparent distortion of the surface at angles greater than about 50° from the 1-3 plane. An example of the experimental data which is analyzed at large angles θ is given in Fig. 7. For positive θ, the mass of the carriers on the nonprincipal surfaces is large enough so that oscillations due only to the principal ellipsoid are observed. For negative θ, beating between the two branches (Fig. 6) occurs, so that in this region the analysis for each period is subject to some uncertainty. It was not possible to determine with any certainty the rate of increase of this distortion with increasing electron concentration, although the same qualitative behavior was observed in several samples. The tilt of the constant energy surfaces was $6°\pm1°$ in all cases.

A number of measurements were taken with **H** in the trigonal plane, and a representative set of results are shown in Fig. 8. We always observed that the ratio of the two periods observed with **H** parallel to a bisectrix axis was very close to 2:1, as is the case in pure bismuth. Since two periods always contribute to the data taken with **H** in the trigonal plane, analysis is not straightforward. However no significant deviations (cf. **H** in binary plane) from the ENP model were observed. The ENP and NENP models are equivalent over this particular angular range but the former provides more tractable theoretical expressions. We may reconcile these observations by postulating that the distortion occurring near the extremities of the surface along the 2 axis is more pronounced near the 2-3 axis. We have sketched in Fig. 6 a cross section of the surface in a 1-3 plane which makes clear the proposed effect. It may be noted that single, beatlike minima in our experimental recordings were often observed when **H** was close to the bisectrix axis. It was never possible to determine a period from the beat since insufficient minima were ob-

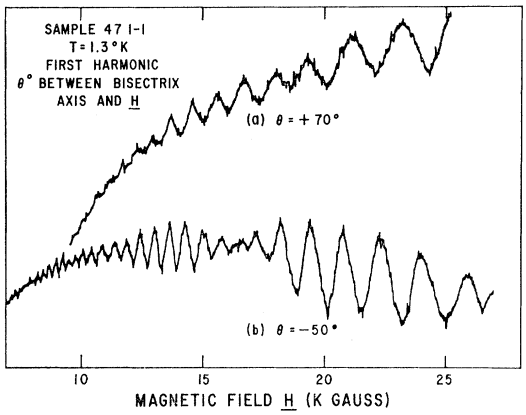

FIG. 7. Photograph of an x-y recording of $\partial R/\partial H$ with the direction of **H** making an angle θ with a bisectrix axis in a binary plane (sign convention as in Fig. 6). For positive θ a single period predominates (a) while for negative θ beating occurs between the two branches shown (b) in Fig. 6.

served. The effect can, however, be explained in a qualitative way by supposing that the distortion gives rise to two extremal areas which can then give rise to a (long period) beat. We also have evidence from measurements of the volume enclosed by the surfaces, that there may be considerable distortion at high electron concentrations near the extremities of the surfaces along the 2 axis.

Although it is not possible to determine m^* for a general direction of **H** in the trigonal plane, values were found for a number of samples with H parallel to a binary axis. In this orientation only a single oscillatory period is observed below 30 kG. To a very good approximation[19]

$$m_{\rm bis}^*/m_{\rm bin}^* \propto \cos\theta\,,$$

where θ is the angle between a binary and a bisectrix axis, viz., 30°. For all samples studied, this relation was found to be valid to within 5%.

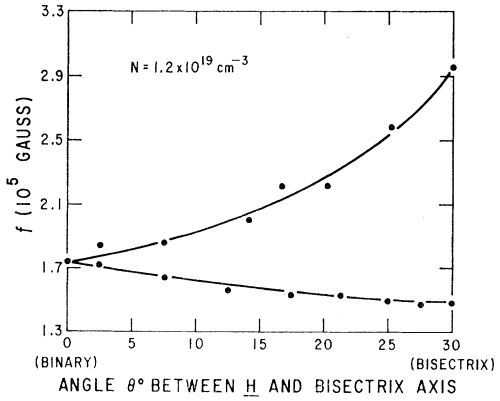

FIG. 8. Angular variation of f with **H** rotated in the trigonal plane. The solid lines are theoretical curves derived from the ENP or the NENP model. Electron concentration 1.2×10^{19} cm^{-3}.

DISCUSSION

In order to discuss the apparent deviations shown in Figs. 4 and 5, it is very desirable to present the data so as to show both f and m^* as functions of the Fermi energy. However, we cannot determine E_f directly from our results without the assumption of a particular band model. Values of E_f calculated from Eqs. (A3)–(A5) are shown in Table I and only below about 65 meV are they seen to be consistent within the experimental uncertainty. Because of the success of the NENP formulation at low energies, we have attempted to describe our results by using a modification of Cohen's model which will be described in the following paragraph. We find that this approach leads to satisfactory agreement with experiment while introducing a minimum of complexity. For example, we have considered more complex dispersion relations,[21,22] but we believe that this approach is not justified at present.

It is now assumed that the quantities m_i, the so-called masses at the band edge, may change with doping. Normally the m_i are constants, predicted by the particular band model. In our model, then, the value of the Fermi energy should be given only by the ratio of f/m^* which is independent of the m_i [see Eq. (A5)]. The same assumption has been used recently to provide a consistent explanation of additional electron bands in bismuth.[11] The results of Figs. 4 and 5 are replotted in Figs. 9 and 10, indicating their dependence on energy measured from the band edge. The solid curves are calculated from Eqs. (A3) and (A4). Note that both f and m^* are underestimated by approximately the same amount. In the $\mathbf{k}\cdot\mathbf{p}$ band theory which was applied to bismuth by Lax and Cohen, the quantities m_i may be written[23]

$$m_i \propto E_g/P^2\,,$$

where E_g is the energy gap at L and P^2 is a momentum

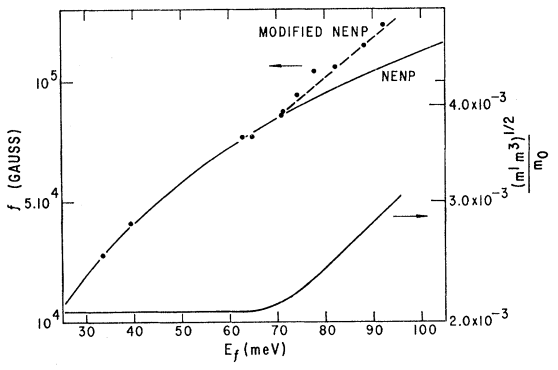

FIG. 9. Frequency f as a function of Fermi energy E_f determined by experimental values of f/m^*. Our modification to the simple NENP theory (dashed curve) is to allow the value of $(m_1m_3)^{1/2}$ to increase with E_f as indicated.

[21] J. O. Dimmock, MIT Lincoln Laboratory Quarterly Report No. 1, 1964, p. 41 (unpublished).
[22] G. A. Baraff, Phys. Rev. **137**, A842 (1965).
[23] E. O. Kane, J. Phys. Chem. Solids **1**, 249 (1957).

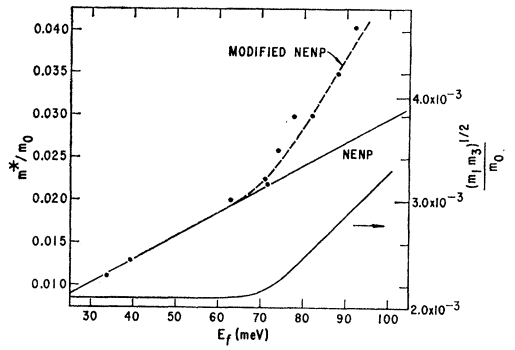

FIG. 10. Effective mass as a function of E_f determined by experimental values of f/m^*. Our modified NENP theory (dashed curve) is obtained by allowing $(m_1m_3)^{1/2}$ to increase with E_f as indicated. The variation of $(m_1m_3)^{1/2}$ is the same as used in Fig. 9.

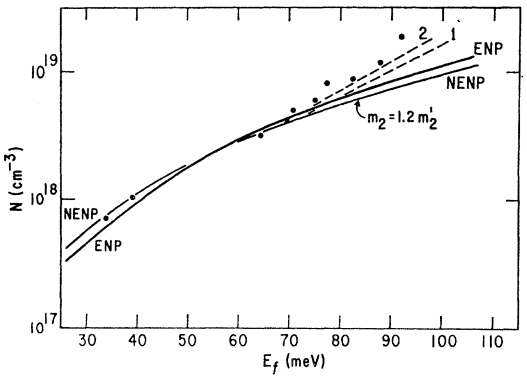

FIG. 11. Variation of electron concentration N with Fermi energy. Theoretical curves for the ENP and NENP ($m_2=1.2\,m_2'$) models are shown. Curve 1 includes the anomolous increase in m_1 and m_3 in the NENP model. Curve 2 assumes an equal increase in m_2.

matrix element. It is not possible to determine values of both P^2 and E_g which would give a unique explanation of our data. If E_g is taken as 15 meV at all Fermi energies, we obtain the modified curves of Figs. 9 and 10 by allowing P^2 to decrease. The resulting increase in m_i [in this case $(m_1m_3)^{1/2}$] with E_f is shown also in Figs. 9 and 10. Note that the same variation of $(m_1m_3)^{1/2}$ is used to fit both the f and m^* results. If P^2 is assumed invariant, it is not possible to account simultaneously for the discrepancy in both f and m^* by increasing E_g with increasing Fermi energy.

We can only speculate at present concerning the mechanism which is responsible for the increase in the m_i. Possibly the occupancy of the higher lying electron bands[11] is important. Cohen *et al.*[24] have advanced arguments which suggest that the energy bands at the L and T points of the zone may be determined, at least in part, by the electron density available in the crystal. In this case the m_i should be regarded as a function of the Fermi energy and this Fermi energy is determined by the electron density. The value of m_i to be used in equations such as (A3) and (A4) must be determined at each Fermi energy before the equations may be applied to deduce the Fermi surface parameters at that energy, that is,

$$S=2\pi(m_1m_3)^{1/2}|_{E=E_f}\times E(1+E/E_g)\,, \tag{1}$$

$$m^*=\partial S/\partial E=(m_1m_3)^{1/2}|_{E=E_f}\times\frac{\partial}{\partial E}[E(1+E/E_g)]. \tag{2}$$

It is obvious from these equations that a given change in $(m_1m_3)^{1/2}$ will be reflected equally in both f and m^*. Recent magneto-optical experiments carried out by Maltz[25] indicate that the NENP model is valid in pure bismuth up to Fermi energies of about 300 meV. This observation does not contradict our proposal that the anomalous behavior described above results from the increased electron concentration. We have also attempted to explain the behavior reported above by taking m_i as a function of energy, viz.,

$$m_0(E)=m_0(0)[1+f(E)].$$

Equations analogous to (1) and (2) may be written as

$$S=2\pi m_0(0)\times E(1+E/E_g)[1+f(E)], \tag{3}$$

$$m^*=m_0(0)\frac{\partial}{\partial E}\left\{E\left(1+\frac{E}{E_g}\right)[1+f(E)]\right\}. \tag{4}$$

We may note that these values of S and m^* will not be changed equally by a given change in $[1+f(E)]$. Our results, therefore, cannot be explained by Eqs. (3) and (4) using any reasonable function $f(E)$.

From Eq. (A2) and the observation that distortion occurs above about 70 meV, we find that $m_2>1.2m_2'$. For the general case where $m_2\neq m_2'$ the volume enclosed by the three equivalent surfaces has been computed numerically. For $m_2=1.2m_2'$, the NENP seriously underestimates the volume (Fig. 11). Curve 1 in this figure is obtained by taking into account the anomalous increase in m_1 and m_3 reported above. Curve 2 includes the effect of an increase in m_2 which is assumed to be of the same magnitude as the experimentally observed change in $(m_1m_3)^{1/2}$. However, a significant discrepancy still remains. It is possible to remove this discrepancy by allowing a much larger increase in m_2 or alternatively to allow an increase in the ratio m_2/m_2' above about 65 meV. This latter implies that distortion sets in more rapidly than predicted by Cohen. Because of the uncertainty associated with the quantitative change in m_2, we cannot determine a unique change in m_2/m_2'. We can say, however, that at $E_f=95$ meV, the value of m_2/m_2' may be as large as 3.5. The angular variation of the area of intersection of the surface described by Eq. (A1) with a plane through the 1 axis (see Fig. 6) has been calculated with m_2/m_2' as a parameter using an IBM 7044 computer. Although a detailed comparison

[24] M. H. Cohen, L. M. Falicov and S. Golin, IBM J. Res. Develop. 8, 215 (1964).
[25] M. Maltz (private communication).

of the distortion predicted for $m_2/m_2'>1$ and that reported above is not possible, we find that over the angular range where measurements are possible there is essentially no difference between the cases $m_2/m_2'=1.00$ and 1.20. To account for the magnitude of the distortion shown in Fig. 4, the value of m_2/m_2' must be 3.5 ± 0.5. Several authors[26,27] have recently reported results which imply $m_2/m_2'\gg1$. These measurements were made by the Shubnikov–de Haas technique applied to Bi-Sb alloys and dilute Bi-Sn. It is difficult to reconcile these results completely with those described in this paper and elsewhere[7] which imply $m_2\simeq m_2'$. Possibly the impurity concentration required to probe the valence band at L in these two alloy systems is sufficient to cause a drastic change in the band itself. A more reasonable explanation of these recent experiments may well be that the Cohen model is just not sufficiently general to describe simultaneously both the conduction and valence band at L.[28]

Finally, we show that the decreasing electron mobility in our doped samples is consistent with the proposed modifications to the NENP model. For ellipsoid surfaces, in the notation of Ref. 29, the mobility is given by

$$\mu\propto\frac{1}{k}\frac{dE}{dk}\left(\frac{1}{N}\frac{1}{k^2}\frac{dE}{dk}\frac{1}{|M(k)|^2}\right)_{E=E_f}. \tag{5}$$

Since μ will be determined by the low mass carriers, this equation should apply to both the ENP and NENP models. Above about 6×10^{17} electrons cm^{-3}, the NENP formulation predicts that $\mu\propto N^{-0.6}$. A line of slope -0.6 is shown in Fig. 2 and it is seen that the fit to experiment is not good. However, the anomalous increase in mass reported above will act to decrease the mobility more rapidly than would be predicted. The dashed line in Fig. 2 shows the theoretical curve including this effect and we see that the agreement with experiment is now satisfactory.

ACKNOWLEDGMENTS

We gratefully acknowledge the valuable contribution made to this work by N. G. Einspruch. Thanks are due also to G. R. Cronin and D. Thompson for providing the bismuth crystals and to D. R. Powell and J. C. Hooper for the numerical computation. Valuable technical assistance was provided by P. J. May and D. W. Attaway.

APPENDIX

We list here the relevant theoretical expressions which have been proposed to describe the bismuth conduction band. In his pioneering measurements, Shoenberg[30] used a three-ellipsoidal model with parabolic energy bands. Because of the small energy gap at the L point of the zone, the conduction band should be highly nonparabolic[5] (ENP model). The high value of m_2 derived experimentally may imply that the ellipsoids are distorted[3] (NENP model).

The general form of the Fermi surface in Cohen's notation[3] for a band centered at L is given by an expression of the form

$$\frac{p_1^2}{2m_1E_g}+\frac{p_3^2}{2m_2E_g}=\left(\frac{E}{E_g}-\frac{p_2^2}{2m_2E_g}\right)\left(1+\frac{E}{E_g}+\frac{p_2^2}{2m_2'E_g}\right), \tag{A1}$$

where m_i are the so-called masses at the bottom of the conduction band and m_i' are the corresponding quantities at the top of the valence band at L. E_g is the energy gap at L. The term in p_2^4 acts to distort the surface at large p_2 values. The areas of the normal sections may increase with p_2 near $p_2=0$ if the following condition is fulfilled

$$m_2/m_2'>1;\quad E_g/E<(m_2/m_2'-1). \tag{A2}$$

This is therefore a condition for the surface to become reentrant.

The cross sectional area and effective mass with **H** parallel to a bisectrix axis is given in the NENP and ENP model by equations of the form

$$S=2\pi(m_1m_3)^{1/2}E(1+E/E_g) \tag{A3}$$

$$m^*=\partial S/\partial E=(m_1m_3)^{1/2}(1+2E/E_g). \tag{A4}$$

Therefore

$$S/2\pi m^*=\frac{E(1+E/E_g)}{1+2E/E_g}. \tag{A5}$$

The total volume enclosed by the three ellipsoids is

$$\text{ENP};\ N=16\pi/h^3(2m_1''m_2''m_3'')^{1/2}E^{3/2}(1+E/E_g)^{3/2}, \tag{A6}$$

$$\text{NENP};\ N=\frac{16\pi}{h^3}(2m_1m_2m_3)^{1/2}E^{3/2}\left(1+\frac{6}{5}\frac{E}{E_g}\right). \tag{A7}$$

The values of m_i'' are derived from the ENP model. However, $m_1=m_1''$ and $m_3=m_3''$.

The volume predicted by the NENP model with $m_2\neq m_2'$ has been numerically evaluated from Eq. (A1) using an IBM 7044 computer.

[26] M. R. Ellet, R. B. Horst, L. R. Williams, and K. F. Cuff, J. Phys. Soc. Japan Suppl. **21**, 666 (1966).

[27] R. T. Bate (private communication).

[28] An alternative explanation of our results may be found by the following reasoning. As the quasiellipsoids become distorted, a second extremal cross section will develop at some finite value of p_2. We have, however, no conclusive evidence for any interaction between the frequencies due to these areas for $H\|$bisectrix axis. Nevertheless if the $p_2\neq0$ cross sections are preferred in the more heavily doped samples, then in such samples the experimental data for $H\|$bisectrix will no longer measure the "waist" of the ellipsoid. However, we can at present think of no good reason why such behavior would occur.

[29] H. Kunze, Phys. Letters **20**, 469 (1966).

[30] D. Shoenberg, Proc. Roy. Soc. (London) **A170**, 341 (1939); Phil. Trans. Roy. Soc. London **A245**, 1 (1952).